

Artificial detection of lower frequency periodicity in climatic studies by  
wavelet analysis demonstrated on synthetic time series

**Running head:** Wavelet artificial detection of periodicity in climatic  
studies

Assaf Hochman<sup>1,2</sup>, Hadas Saaroni<sup>2</sup>, Felix Abramovich<sup>3</sup>, Pinhas Alpert<sup>1</sup>

<sup>1</sup> Department of Geophysics, Porter School of the Environment and Earth Sciences,  
Tel-Aviv University, Tel-Aviv, Israel, 69978

<sup>2</sup> Department of Geography and the Human Environment, Porter School of the  
Environment and Earth Sciences, Tel-Aviv University, Tel-Aviv, Israel, 69978

<sup>3</sup> Department of Statistics and Operations Research, School of Mathematical Sciences,  
Tel-Aviv University, Tel-Aviv, Israel, 69978

Submitted to: Journal of Applied Meteorology and Climatology

**Corresponding author:**

Assaf Hochman<sup>1, 2, 3</sup>

E-mail- [assafhochman@yahoo.com](mailto:assafhochman@yahoo.com)

1 **Abstract**

2 The Continuous Wavelet Transform (CWT) is a frequently used tool to study  
3 periodicity in climate and other time series. Periodicity plays a significant role in  
4 climate reconstruction and prediction. In numerous studies, the use of CWT revealed  
5 Dominant Periodicity (DP) in climatic time series. Several studies suggested that these  
6 "natural oscillations" would even reverse global warming. It is shown here that the  
7 results of wavelet analysis for detecting DPs can be miss-interpreted in the presence of  
8 local singularities that are manifested in lower frequencies. This may lead to false DPs  
9 detection. In CWT analysis of synthetic and real-data climatic time series, with local  
10 singularities, CWT indicates on a low frequency DP even if there is no true periodicity  
11 in the time series. It is argued that this is an inherent general property of CWT. Hence,  
12 applying CWT to climatic time series should be re-evaluated and more careful analysis  
13 of the entire wavelet power spectrum is required, focusing on high frequencies as well.  
14 Thus, a cone-like shape in the wavelet power spectrum most likely indicates the  
15 presence of a local singularity in the time series rather than a DP, even if the local  
16 singularity has an observational or a physical basis. It is shown that analyzing the  
17 derivatives of the time series may be helpful in interpreting the wavelet power spectrum.  
18 Nevertheless, this is only a partial remedy that does not completely neutralize the effects  
19 caused by the presence of local singularities.

20

21 **Keywords:** Wavelet analysis, climate time-series, climate change, mother wavelet,  
22 Morlet, artificial periodicity, Fast Fourier Transform

23

24

25

26

27

28

29

30

31

32

33

## 1 **1. Introduction**

2 Spectral methods such as the Continuous Wavelet Transform (CWT, frequently  
3 named wavelet analysis) and the Fast Fourier Transform (FFT) have a special appeal  
4 for climate and paleo climate research because they can be used to detect periodicities  
5 in time series and other applications. CWT has therefore become a most common tool  
6 for the study of variations within climate time series, capable to analyse them with  
7 different timescales, which is imperative in climate reconstruction and prediction  
8 (Torrence and Compo, 1998). An appealing feature of CWT is its ability to analyse  
9 non-stationary time series, which is vital in climate research (Lau and Weng, 1995).

10 Recently, CWT was used in a plethora of climate and geophysical studies (e.g., Gray  
11 *et al.*, 2004; Knight *et al.*, 2005; Li *et al.*, 2011; DeLong *et al.*, 2012; McCabe-Glynn *et al.*  
12 *et al.*, 2013; Pike *et al.*, 2013; Cox *et al.*, 2014; Duan *et al.*, 2014; Kreppel *et al.*, 2014;  
13 Magee *et al.*, 2014; Soon *et al.*, 2014; Xu *et al.*, 2014; Burn *et al.*, 2015; Lee *et al.*,  
14 2015; Wright *et al.*, 2015; Novello *et al.*, 2016; Sharma *et al.*, 2016). These studies have  
15 incorporated CWT as a primary tool, chosen from the many other signal analysis tools  
16 within the frequency domain. These authors have highlighted Dominant Periodicity  
17 (DP) in climatic, paleo climatic and geophysical time series, attributing them to natural  
18 origin (e.g., NAO, ENSO, PDO, solar cycles, solar irradiance, thermohaline circulation,  
19 etc.). Cone like shapes, expressing low frequency DPs in the wavelet power spectrum  
20 that emerged in the aforementioned studies have motivated the present work. It is  
21 stressed that low frequency DPs may suggest a long term climatic process as opposed  
22 to local high frequency features. Thus, low frequency DPs are appealing in improving  
23 predictability of the climate system.

24 Frequently, such studies detected DP's using a point wise significance testing  
25 procedure applied to the wavelet spectrum (Torrence and Compo, 1998). These authors  
26 have suggested that for a first order auto-regressive process with lag-1 auto-correlation,  
27 a theoretical normalized red-noise power spectrum can be computed. To obtain the 5%  
28 significance level, the red-noise power spectrum is multiplied by the 95% of a chi-  
29 square distribution with two degrees of freedom and then the result is divided by two  
30 to remove the degrees of freedom factor. The auto-correlation coefficient can be  
31 estimated by standard methods, e.g., Allen and Smith (1996) used in this study.

32 DPs are defined herein as a statistically significant region of the wavelet spectrum  
33 within a band of lower frequencies/periodicities (e.g., Figure 1). It is emphasized that  
34 these higher power regions extend in time and are not very local features in the power

1 spectrum. As such, many climatic studies relate DPs to natural cycles of the climate  
2 system, as indicated above. However, point wise testing procedures applied to  
3 simultaneous testing of a large number of wavelet coefficients ignore the severe  
4 multiple testing problem and, therefore, typically result in detection of spurious patches  
5 in the wavelet power spectrum (e.g., Abramovich and Benjamini, 1995; Maraun *et al.*,  
6 2007). When one performs a test at a specific significance level, by definition one  
7 rejects the null hypothesis at a certain percent (e.g., 5%) even if it is true. Thus, when  
8 performing a test many times, a certain percent would emerge as spuriously significant.  
9 This is referred to as the multiple testing problem mentioned above (Maraun and  
10 Kurths, 2004). Nevertheless, pointwise significance testing is still the most commonly  
11 used significance test in climate studies.

12 Several improved significance testing procedures were considered in the literature.  
13 Maraun *et al.* (2007) proposed an area wise significance test. The main disadvantage of  
14 this test is the complexity of the significance level calculation, which involves a root-  
15 finding algorithm. Liu *et al.* (2007) have addressed the bias problem in the estimate of  
16 the wavelet spectra in atmospheric and oceanic datasets. They have suggested a  
17 rectification procedure, which is the transform coefficient squared divided by the scale  
18 it associates with. Schulte *et al.* (2015) developed a Geometric method for significance  
19 testing in the wavelet domain. It was found that this method produces results similar to  
20 the area wise significance test (Schulte *et al.*, 2015) while being more computationally  
21 flexible and efficient. In a most recent study, the Geometric method was improved by  
22 a cumulative area wise significance testing procedure (Schulte, 2016). It was shown  
23 that the latter test implies higher statistical power in most cases, especially when the  
24 signal-to-noise ratio is high (Schulte, 2016).

25 The purpose of this paper is to show that the CWT, even after applying the  
26 aforementioned state-of-the-art methods, still often identifies artificial lower frequency  
27 DPs arising from local singularities in a time series that can lead to misinterpretation of  
28 the wavelet power spectrum. This observation is particularly important because of the  
29 enormous recent increase in the number of publications using wavelet analysis in  
30 climate research, from 15 publications per year in 1998 to about 550 in 2018 (Science  
31 Direct).

32

## 33 **2. Data and methods**

1 To demonstrate the detection of artificial DPs in the wavelet power spectrum we  
2 applied the state-of-the-art Cumulative Area Wise (Schulte, 2016) and the Geometric  
3 (Schulte *et al.*, 2015) significance testing procedures  
4 ([www.mathworks.com/matlabcentral/fileexchange/](http://www.mathworks.com/matlabcentral/fileexchange/)) to six synthetic and four real  
5 climate time series:

- 6 1) A sine time series with a ~200 low frequency periodicity (Figure 1).
- 7 2) The sun-spot number time series (SILSO, World Data Center; Figure 2).
- 8 3) A local abrupt change (step) time series generated manually (Figure 3).
- 9 4) Stratospheric aerosol optical depth time series (Bourassa *et al.*, 2012; Figure 4).
- 10 5) A red noise time series (Figure 5).
- 11 6) The local abrupt change time series added to the red noise time series (Figure 6).
- 12 7) The sine time series added to the red noise time series (Figure 7).
- 13 8) The Pacific Decadal Oscillation (PDO) reconstruction (Mann *et al.*, 2009; Figure  
14 8).
- 15 9) The daily Nino3.4 index for 12.7.2015 – 6.4.2018 (Reynolds *et al.*, 2007; Figure  
16 9).
- 17 10) A time series containing a few local abrupt changes added to red noise (Figure  
18 10).

19 For all the examples, we applied the above advanced significance testing procedures  
20 of Schulte *et al.* (2015) and Schulte (2016), where we used the Morlet 6 "mother"  
21 wavelet, which is the most commonly used wavelet in geophysics. All time series were  
22 padded with zeros at the edges as typically recommended in geophysics. We used a red  
23 noise (see introduction) and the applied significance testing procedure were adapted  
24 correspondingly to such a noise background, by generating 1000 realizations of noisy  
25 samples from this surrogate distribution, using Monte-Carlo techniques. Red noise is  
26 a commonly used background in geophysics (Torrence and Compo, 1998; Maraun *et al.*  
27 *et al.*, 2007; Schulte *et al.*, 2015; Schulte, 2016). It is noted that the null distribution (the  
28 time series is similar to a red-noise background) of the normalized area of a significance  
29 patch depends on the choice of null hypothesis, with, for red-noise processes, the  
30 normalized area increases with increasing lag-1 autocorrelation coefficients (Schulte *et al.*  
31 *et al.*, 2015).

32 For the sake of comparison, the Fast Fourier Transform, and pointwise wavelet  
33 significance testing (Torrence and Compo, 1998) were also applied to the time series  
34 described above (Figure S1, S2, respectively). The bias rectification procedure (Liu *et*

1 *al.*, 2007) was further applied to the synthetic time series before using the Cumulative  
2 Area Wise significance test (Schulte 2016; Figure S3). In addition, boundary conditions  
3 may be a considerable source of uncertainty in climate and other time series. Several  
4 options have been presented in the literature. For example, Lin and Franzke (2015) and  
5 Gallegati (2018) have extended their time series using a symmetric/anti-symmetric  
6 extension mode. No clear recommendation has yet been given for climate time series.  
7 Here, the effect of using zero padding is evaluated for the synthetic time series (Figure  
8 S4). We have further investigated the above mentioned time series using alternative  
9 "mother" wavelets including the Paul (Figure S5) and Dog (Figure S6) "mother"  
10 wavelets.

11 To better distinguish between real DPs and local abrupt changes, it may be helpful  
12 to apply wavelet-based tests to the derivative (the rate of change at each time step) of  
13 the original time series. Taking the derivative does not affect periodicity. On the other  
14 hand, it reduces regularity of a signal, and a local singularity would be stronger  
15 manifested at higher frequencies of the wavelet spectrum. See Mallat (2008, Section 6)  
16 for rigorous mathematical analysis.

17

### 18 **3. Results**

19 CWT should only detect periodicities in the Sine time series (Figure 1), in the sun-  
20 spot number time series (Figure 2; SILSO, World Data Center), and in the Sine time  
21 series with red noise (Figure 7) as shown in the Fast Fourier Transform analysis (Figure  
22 S1). However, the wavelet power spectrum indicates the presence of DPs in all  
23 considered time series (Figures 1-10). The detected periodicities in the wavelet power  
24 spectrum in Figures 3-6 and 8-10 are artificial and are caused by local abrupt changes  
25 in the time series. It should be stressed that local abrupt changes may represent a real  
26 physical change in the system. For example, the stratospheric aerosol optical depth  
27 attributed to volcanic eruptions is analyzed here (Figure 4; Bourassa *et al.*, 2012). Two  
28 major local abrupt changes that coincide with the large volcanic eruptions of Krakatoa  
29 in 1883 and of El Chicon and Mount Pinatubo in 1982 and 1991, respectively, produce  
30 DPs at the 10-12 year periods (Figure 4). The CWT accurately detects the local abrupt  
31 change location on high frequency scales (Figures 3c, e – 10c, e). However, in the  
32 lower frequencies, the patch expands in time (Figures 3c, e – 10c, e) and results in a  
33 lower frequency band in the wavelet power spectrum, that may be erroneously  
34 interpreted as indication of a DP in the time series. Furthermore, it seems that the

1 Cumulative Area Wise test is more susceptible to the emergence of lower frequency  
2 DPs than the Geometric test (Figures 3c, e – 10c, e).

3 Following our remarks at the end of Section 2, we analyzed also the wavelet  
4 spectrum of the original time series derivative. Figure 1d, f and 2d, f show that the  
5 derivative of the Sine time series and the sun-spot number time series, respectively,  
6 indeed leaves the low frequency periodicity intact. On the other hand, when there are  
7 local abrupt changes in the time series (e.g., Figure 6 and 10), using the derivative  
8 emphasizes the power at higher frequencies in the wavelet power spectrum and reduces  
9 the power in the lower frequency patches (Figure 6d, f and 10d, f). However, it still  
10 does not completely prevent detection of false DPs. This is further demonstrated in real  
11 reconstructed PDO and Nino3.4 time series (Figure 8d, f and 9d, f). Thus, using the  
12 derivatives is a partial remedy that does not completely neutralize the effects caused by  
13 the presence of local singularities.

14 It is further shown that the pointwise significance testing procedure (Torrence and  
15 Compo, 1998) also displays significant artificial low frequency DPs in the  
16 aforementioned time series (Figure S2). This test mostly does not find the high  
17 frequency scales as significant, in contrast to the area based tests (Schulte *et al.*, 2015;  
18 Schulte 2016).

19 Rectifying the wavelet power spectrum may allow the comparison of spectral peaks  
20 across scales (Liu *et al.*, 2007). However, for time series containing local abrupt  
21 changes, the Cumulative Area Wise significance test (Schulte 2016) finds the high  
22 frequency scales as significant but not the real DPs (Figure S3).

23 Figure S4 displays the effect of using zero padding on the synthetic time series used  
24 in this study. It is shown that using the zero padding procedure (Figure S4 left column)  
25 reduces boundary conditions in all aforementioned time series with respect to no  
26 padding (Figure S4 right column). It is stressed that zero padding is helpful wherever it  
27 smooths the time series at its boundaries, thus reducing the effect of local singularities.  
28 For example, the improvement in the boundary conditions is higher in the left side of  
29 the sine time series than in the right side (Figure S4a, b, respectively). Thus, no clear  
30 recommendation can be given for climate time series since the edge effects will highly  
31 depend on the analyzed time series edges. It is recommended to analyze time series  
32 with different extension procedures to give a better evaluation of edge effects.

33 Finally, it is found that the Morlet 6 "mother" wavelet is the least susceptible to the  
34 effect of local singularities on lower frequency DPs (Figures 1-10) with respect to the

1 Paul (Figure S5) and Dog (Figure S6) "mother" wavelets. Thus, we recommend using  
2 Morlet 6 for climate time series as earlier recommended (Torrence and Compo, 1998;  
3 Maraun *et al.*, 2007; Schulte *et al.*, 2015; Schulte, 2016).

4 Summarizing, we argue that local singularities, commonly present in climatic time  
5 series (e.g., Yosef *et al.*, 2018) can induce low-frequency power that may be interpreted  
6 as DPs. It is further stressed here that spectral methods have been used to quantify non-  
7 linearity in time series (May 1976). Such non-linearity can lead to abrupt changes in  
8 time series and in turn, period doubling bifurcations that will ultimately be exhibited as  
9 a cone like shape in the wavelet power spectrum (Weng and Lau, 1994).

10 We have demonstrated this problematic feature on synthetic time series and on real  
11 climatic series. However, it should be noted that any series containing local singularities  
12 would necessarily produce a DP at lower frequencies, as this is inherent to wavelet  
13 analysis (Holschneider 1995; Abramovich *et al.*, 2000; Mallat 2008).

14

15 **4. Discussion**

16 The results of using CWT for detecting periodicities in climate time series might be  
17 misleading, as demonstrated here on different synthetic as well as real climate time  
18 series. It is shown that the presence of a lower frequency band in the wavelet power  
19 spectrum does not necessarily indicate a real periodicity, but is often caused by local  
20 singularities in the time series (as shown in Figures 3-6 and 8-10). Note that one can  
21 think of CWT as a series of localized band-pass filters, where low frequencies  
22 correspond to large windows in the time domain. Therefore, local singularities would  
23 be necessarily manifested in the lower frequencies domain of the wavelet power  
24 spectrum (Holschneider, 1995; Abramovich *et al.*, 2000; Mallat, 2008). A finer analysis  
25 of the geometry of patch shapes is required to distinguish between a true DP and an  
26 abrupt change in a time series. The latter typically yields local maxima within a cone  
27 around its location that propagate along high frequencies in the wavelet spectrum (e.g.,  
28 Mallat, 2008, Sections 6.1-6.2), while DPs are characterized by temporally long bands  
29 in the low frequency domain. In this case, one could think of some length test for a  
30 patch. The problem, however, is more challenging, as there is occasionally a series of  
31 local singularities with interfering cones that might look similar to a long band in the  
32 low frequency domain (Figures 8-10). Here, we suggest to use the derivative of a time  
33 series as an additional test to distinguish between real periodicity and low frequency



1 bands in the wavelet power spectrum emerging from local singularities. However, it  
2 still does not completely prevent detection of false DPs.

3 Summarizing, in order to distinguish between various possible scenarios, a  
4 topological analysis of the entire wavelet power spectrum is required, focusing on high  
5 frequency as well. Accordingly, whenever a lower frequency dominant periodicity  
6 appears in the wavelet power spectrum, one should also analyze the higher frequency,  
7 to distinguish between a real periodicity and an artificial one, produced by local  
8 singularities. Cone-like shapes in the wavelet power spectrum, propagating from the  
9 higher to the lower frequencies, most likely indicate on an artificial DP. The rigorous  
10 theory for such an analysis is a topic for further research.

11

## 12 **Acknowledgements**

13 This study was partly supported by the Tel-Aviv University (TAU) President and  
14 Mintz foundation, and by the Porter School of Environmental Studies at TAU. This  
15 study was also partially supported by cooperation in the international virtual institute  
16 DESERVE (Dead Sea Research Venue), funded by the German Helmholtz Association  
17 and the Israel Science Foundation (ISF 1123/17) and the Mediterranean Sea Research  
18 Center of Israel (MERCID). We would like to thank Prof. Amir Averbuch and Prof.  
19 Valeri Zheludev for most useful discussions regarding the basics of wavelet analysis  
20 methodology (Averbuch *et al.*, 2014, 2015).

21

## 22 **References**

- 23 Abramovich F, Benjamini Y. 1995. Thresholding of wavelet coefficients as multiple  
24 hypotheses testing procedure. In *Wavelets and Statistics* (Eds. Antoniadis, A. and  
25 Oppenheim, G.), Lecture Notes in Statistics 103, Springer--Verlag, pp. 5-14.
- 26 Abramovich F, Bailey TC, Sapatinas T. 2000. Wavelet  
27 analysis and its statistical applications. *Journal of the Royal Statistical Society series*  
28 **D (The Statistician) 49**: 1-29.
- 29 Allen MR, Smith LA. 1996. Monte Carlo SSA: Detecting irregular oscillations in the  
30 presence of colored noise. *Journal of Climate* **9**: 3373–3404.
- 31 Averbuch AZ, Neittaanmäki P, Zheludev VA. 2014. *Spline and Spline Wavelet*  
32 *Methods with Applications to Signal and Image Processing Volume 1: Periodic*  
33 *Splines*. Springer international publishing Switzerland, 496pp.

- 1 Averbuch AZ, Neittaanmäki P, Zheludev VA. 2015. Spline and Spline Wavelet  
2 Methods with Applications to Signal and Image Processing Volume 2: Non Periodic  
3 Splines. Springer international publishing Switzerland, 426pp.
- 4 Burn MJ, Palmer SE. 2015. Atlantic hurricane activity during the last millennium.  
5 *Scientific Reports*. DOI: 10.1038/srep12838
- 6 Bourassa AE, Robock A, *et al.* 2012. Large volcanic aerosol load in the stratosphere  
7 linked to Asian monsoon transport. *Science* **337**: 78-81,  
8 DOI:10.1126/science.1219371
- 9 Cox CJ, Walden VP, Compo GP, Rowe PM, Shupe MD, Steffan K. 2014. Downwelling  
10 longwave flux over summit, Greenland, 2010-2012: analysis of surface-based  
11 observations and evaluation of ERA interim using wavelets. *Journal of Geophysical*  
12 *Research: Atmospheres* **119**: 12317-12377. DOI:10.1002/2014JD021975
- 13 DeLong KL, Quinn TM, Taylor FW, Lin K, Shen CC. 2012. Sea surface temperature  
14 variability in the southwest tropical Pacific since AD 1649. *Nature Climate Change*  
15 **2**: 799-804.
- 16 Duan F, Wang Y, Shen CC, Wang Y, Cheng H, Wu CC, Hu HM, Kong X, Liu D, Zhao  
17 K. 2014. Evidence for solar cycles in a late Holocene speleothem record from  
18 Dongge Cave, China. *Scientific Reports*. DOI: 10.1038/srep05159
- 19 Gallegati M. 2018. A systematic wavelet-based exploratory analysis of climatic  
20 variables. *Climatic Change* **148**: 325-338. DOI:10.1007/s10584-018-2172-8
- 21 Gray ST, Graumlich LJ, Betancourt JL, Pederson GT. 2004. A tree-ring based  
22 reconstruction of the Atlantic Multidecadal Oscillation since 1567 A.D. *Geophysical*  
23 *Research Letters* **31**: L12205. DOI:10.1029/2004GL019932
- 24 Holschneider M. 1995. Wavelets — an Analysis Tool, Oxford University  
25 Press, Oxford.
- 26 Knight JR, Allan RJ, Folland CK, Vellinga M, Mann ME. 2005. A signature of  
27 persistent natural thermohaline circulation cycles in observed climate. *Geophysical*  
28 *Research Letters* **32**: L20708. DOI: 10.1029/2005GL024233
- 29 Kreppel KS, Caminade C, Telfer S, Rajerison M, Rahalison L, Morse A, Baylis M.  
30 2014. A non-stationary relationship between global climate phenomena and human  
31 plague incidence in Madagascar. *PLOS Neglected Tropical Diseases* **8**: 1-13.
- 32 Lau KM, Weng H. 1995. Climate signal detection using wavelet transform: How to  
33 make a time series sing. *Bulletin of the American Meteorological Society* **76(12)**:  
34 2391-2402.

- 1 Lee HF, Pei Q, Zhang DD, Choi KPK. 2015. Quantifying the intra-regional  
2 precipitation variability in North-Western China over the past 1400 years. *PLOS One*  
3 **10(7)**: e0131693.
- 4 Li J, Xie SP, Cook ER, Huang G, D'Arrigo R, Liu F, Ma J, Zheng XT. 2011. Inter-  
5 decadal modulation of El-Nino amplitude during the last millennium. *Nature*  
6 *Climate Change* **1**: 114-118.
- 7 Lin Y, Franzke CLE. 2015. Scale-dependency of the global mean surface temperature  
8 trend and its implication for the recent hiatus of global warming. *Scientific Reports*  
9 **5**:12971. DOI: 10.1038/srep12971
- 10 Liu YG, San Liang X, Weisberg RH. 2007. Rectification of the bias in the wavelet  
11 power spectrum. *Journal of Atmospheric Ocean Technology* **24**:2093-2102.
- 12 Magee NB, Melaas E, Finocchio PM, Jardel M, Noonan A, Lacono MJ. 2014. Blue  
13 hill observatory sunshine, assessment of climate signals in the longest continuous  
14 meteorological record in North America. *Bulletin of the American Meteorological*  
15 *Society* **95**: 1741-1751.
- 16 Mallat S. 2008. A Wavelet tour on signal processing, third edition: the sparse way  
17 Academic Press.
- 18 Mann ME, Zhihua Z, Rutherford S, Bradley RS, Hughes MK, Shindell D, Ammann C,  
19 Faluvegi G, Ni F. 2009. Global Signatures and Dynamical Origins of the Little Ice  
20 Age and Medieval Climate Anomaly. *Science* **326(5957)** 1256-1260. DOI:  
21 10.1126/science.1177303
- 22 Maraun D, Kurths J. 2004. Cross wavelet analysis: significance testing and pitfalls.  
23 *Non-linear Processes in Geophysics* **11**: 505-514.
- 24 Maraun D, Kurths J, Holschneider M. 2007. Nonstationary Gaussian processes in  
25 wavelet domain: synthesis, estimation, and significance testing. *Physical Review E*.  
26 **75**. DOI: 10.1103/PhysRevE.75.016707.
- 27 May RM. 1976. Simple mathematical models with very complicated dynamics. *Nature*  
28 **261**: 459-475.
- 29 McCabe-Glynn S, Johnson KR, Strong C, Berkelhammer M, Sinha A, Cheng H,  
30 Edwards RL. 2013. Variable North-Pacific influence on drought in South-Western  
31 North America since AD 854. *Nature Geoscience* **6**: 617-621.
- 32 Novello VF, Vuille M, Cruzl FW, Strikis NM, Paula MSD, Edwards RL, Cheng H,  
33 Karmann I, Jaqueto PF, Trindade RIF, Hartmann GA, Moquet JS. 2016. Centennial-

1 scale solar forcing of the South American Monsoon System recorded in stalagmites.  
2 *Scientific Reports*. DOI: 10.1038/srep24762

3 Pike J, Swann GEA, Leng MJ, Snelling MA. 2013. Glacial discharge along the West  
4 Antarctic peninsula during the Holocene. *Nature Geoscience* **6**: 199-202.

5 Reynolds RW, Smith TM, Liu C, Dudley B, Chelton KS, Casey MGS. 2007: Daily  
6 High-Resolution-Blended Analyses for Sea Surface Temperature. *Journal of*  
7 *Climate* **20**: 5473-5496.

8 Schulte JA, Duffy C, Najjar RG. 2015. Geometric and topologic approaches to  
9 significance testing in wavelet analysis. *Non-Linear Processes in Geophysics* **22**:  
10 139-156.

11 Schulte JA. 2016. Cumulative area wise testing in wavelet analysis and its application  
12 to geophysical time series. *Non-Linear Processes in Geophysics* **23**: 45-57.

13 Sharma S, Magnuson JJ, Batt RD, Winslow LA, Korhonen J, Ono YA. 2016. Direct  
14 observations of ice seasonality reveal changes in climate over the past 320–570  
15 years. *Scientific Reports*. DOI: 10.1038/srep25061

16 SILSO, World Data Center - Sunspot Number and Long-term Solar Observations,  
17 Royal Observatory of Belgium, on-line Sunspot Number catalogue:  
18 <http://www.sidc.be/SILSO/>.

19 Soon W, Herrera VMV, Selvaraj K, Traversi R, Usoskin I, Chen CTA, Lou JY, Kao  
20 SJ, Carter RM, Pipin V, Severi M, Becagli S. 2014. A review of Holocene solar-  
21 linked climatic variation on centennial to millennial timescales: Physical processes,  
22 interpretative frameworks and a new multiple cross-wavelet transform algorithm.  
23 *Earth-Science Reviews* **134**: 1-15.

24 Torrence C, Compo GP. 1998. A practical guide to wavelet analysis. *Bulletin of the*  
25 *American Meteorological society* **79**: 61-78.

26 Weng H, Lau KM. 1994. Wavelets, period doubling and time-frequency localization  
27 with application to organization of convection over the tropical west pacific. *Journal*  
28 *of the Atmospheric Sciences* **51(17)**: 2523 - 2541.

29 Wright R, Blackett M, Hill-Butler C. 2015. Some observations regarding the thermal  
30 flux from Earth's erupting volcanoes for the period of 2000 to 2014. *Geophysical*  
31 *Research Letters* **42**: 282-289. DOI:10.1002/2014GL061997

32 Xu D, Lu H, Chu G, Wu N, Shen C, Wang C, Mao L. 2014. 500-year climate cycles  
33 stacking of recent centennial warming documented in an East Asian pollen record.  
34 *Scientific Reports*. DOI: 10.1038/srep03611.

1 Yosef Y, Aguilar E, Alpert P. 2018. Detecting and adjusting artificial biases of long-  
2 term temperature records in Israel. *International Journal of Climatology*  
3 DOI:10.1002/joc.5500.

4  
5 **Legend to figures**

6 **Figure 1** A Sine time series (a) and the derivative of the sine time series (b) Continuous  
7 Wavelet Transform (CWT) applied with (c,d) Cumulative area wise (Schulte 2016) (e,f)  
8 Geometric (Schulte *et al.*, 2015) significance testing using a Morlet 6 "mother" wavelet.  
9 The Wavelet Power Spectrum is shown for both significance testing. The black  
10 contours are regions found to be significant at the 5% level with respect to a red noise  
11 background using 1000 realizations from a Monte Carlo experiment. The shaded  
12 regions mark the cone of influence in which boundary conditions become important.  
13 The Dominant Periodicities (DP) are marked in an arrow. DPs are a statistically  
14 significant region of the wavelet spectrum within a band of lower  
15 frequencies/periodicities. It is emphasized that these higher power regions extend in  
16 time and are not very local features in the power spectrum.

17 **Figure 2** Same as Figure 1 but for the sun-spot number time series (SILSO, World Data  
18 Center). Dominant Periodicities (DP) are marked in arrows.

19 **Figure 3** Same as Figure 1 but for a Local Abrupt Change time series. Local Abrupt  
20 Changes (LAC) and Dominant Periodicities (DP) are marked in arrows.

21 **Figure 4** Same as Figure 1 but for the stratospheric aerosol optical depth time series  
22 (Bourassa *et al.*, 2012). Local Abrupt Changes (LAC) and Dominant Periodicities (DP)  
23 are marked in arrows.

24 **Figure 5** Same as Figure 1 but for a red noise time series.

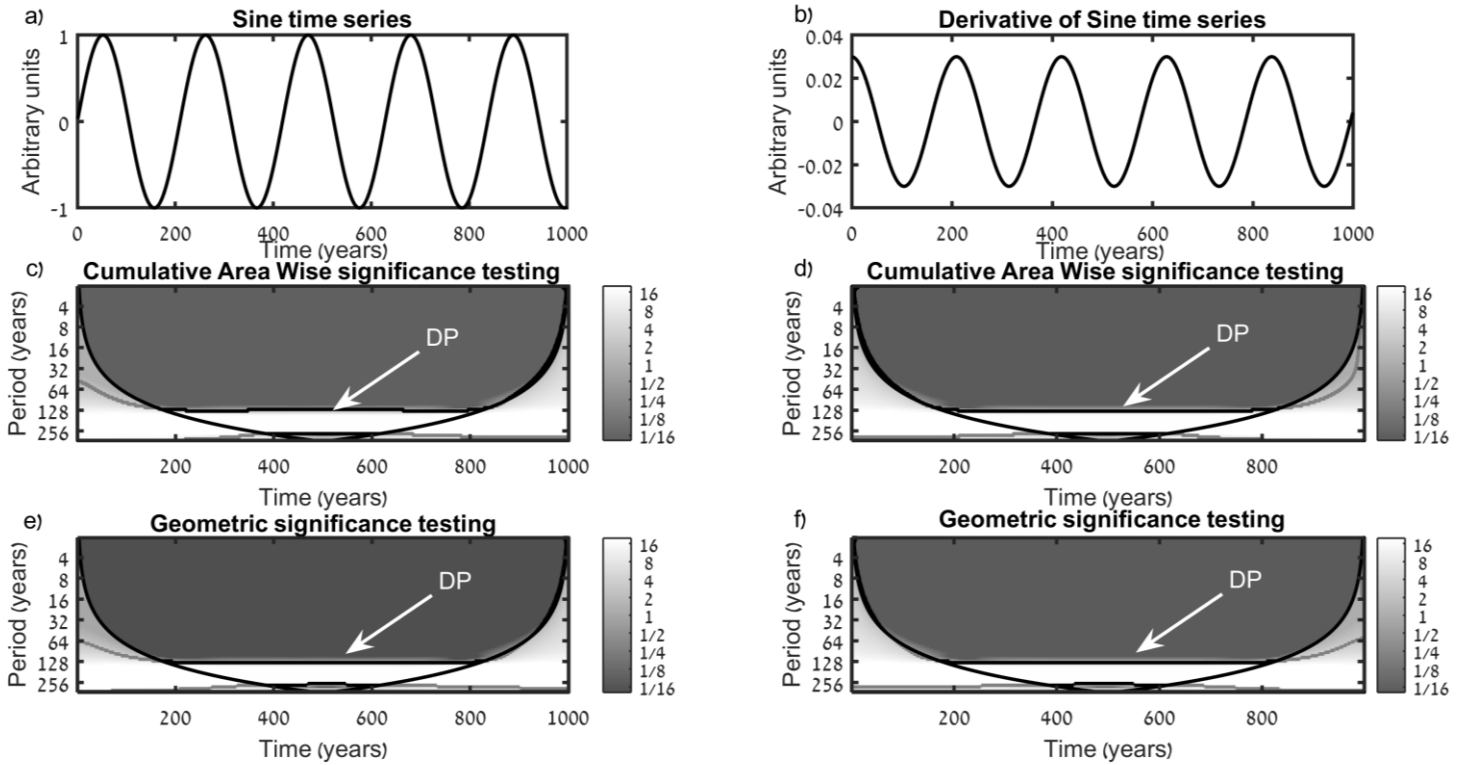
25 **Figure 6** Same as Figure 1 but for the red noise time series added to the Local Abrupt  
26 Change (LAC) time series. LAC and Dominant Periodicities (DP) are marked in arrows.

27 **Figure 7** Same as Figure 1 but for the sine time series added to the red noise time series.  
28 Dominant Periodicities (DP) are marked in arrows.

29 **Figure 8** Same as Figure 1 but for the reconstructed PDO (Mann *et al.*, 2009). Local  
30 Abrupt Changes (LAC) and Dominant Periodicities (DP) are marked in arrows.

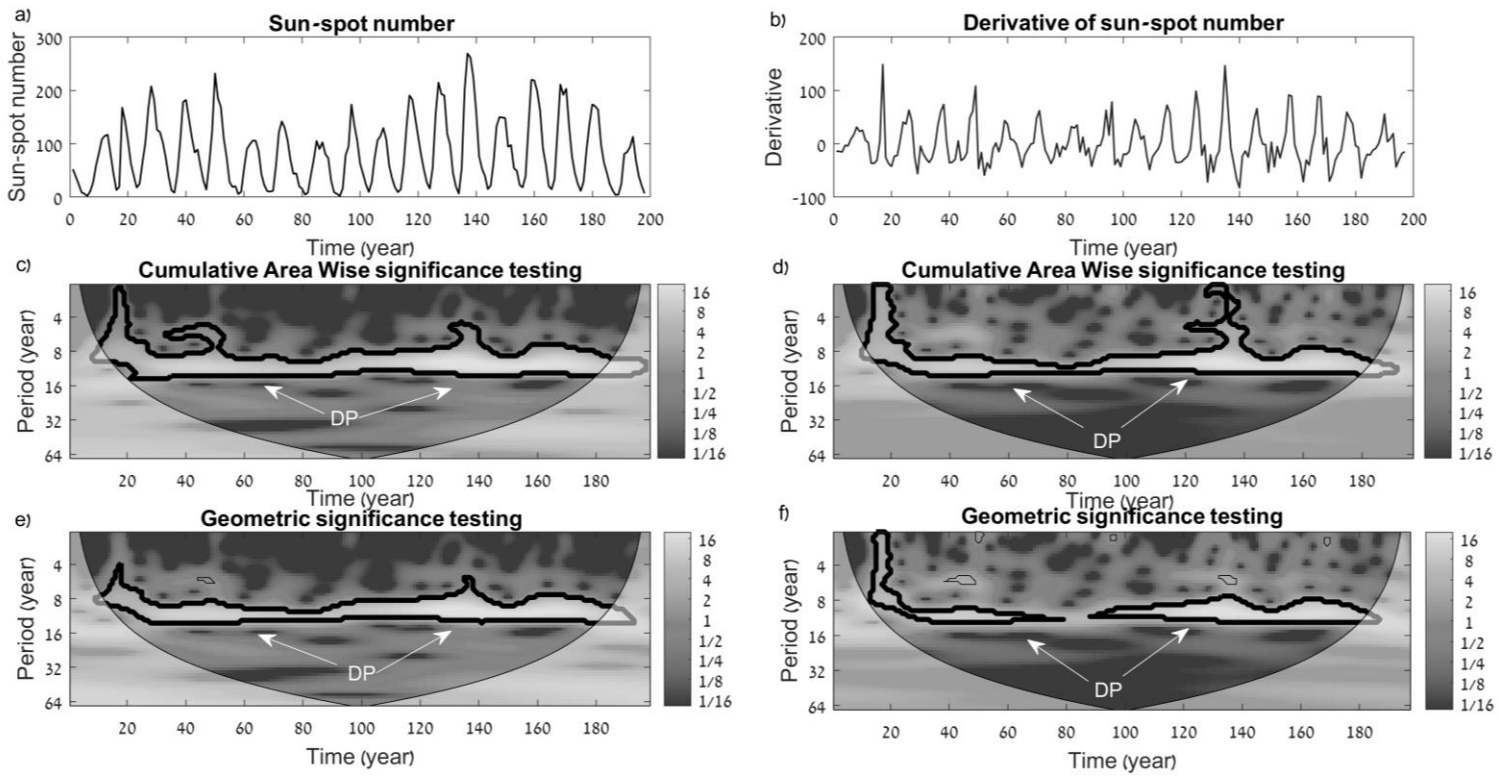
31 **Figure 9** Same as Figure 1 but for the Nino3.4 index 12.7.2015 – 6.4.2018. Local  
32 Abrupt Changes (LAC) and Dominant Periodicities (DP) are marked in arrows.

33 **Figure 10** Same as Figure 1 but for a time series with a few Local Abrupt Changes  
34 (LAC) added to red noise.



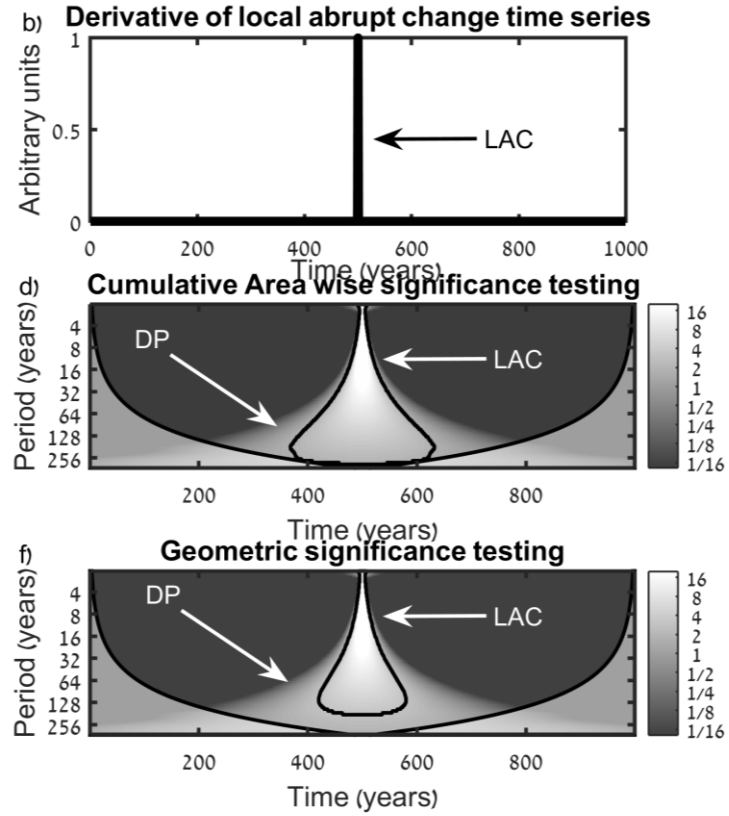
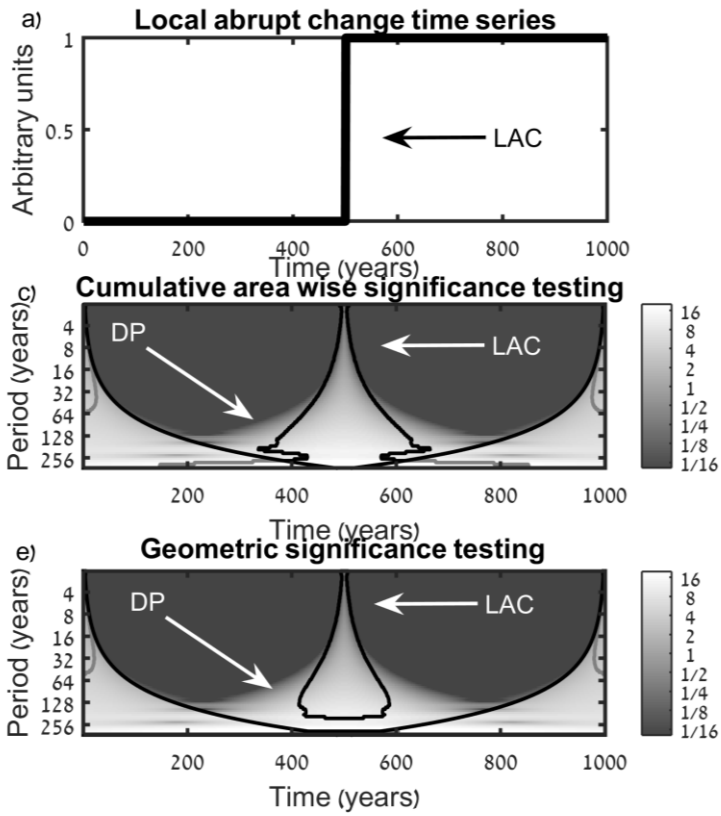
1 **Figure 1** A Sine time series (a) and the derivative of the sine time series (b) Continuous  
 2 Wavelet Transform (CWT) applied with (c, d) Cumulative area wise (Schulte 2016) (e,  
 3 f) Geometric (Schulte *et al.*, 2015) significance testing using a Morlet 6 "mother"  
 4 wavelet. The Wavelet Power Spectrum is shown for both significance testing. The  
 5 black contours are regions found to be significant at the 5% level with respect to a red  
 6 noise background using 1000 realizations from a Monte Carlo experiment. The shaded  
 7 regions mark the cone of influence in which boundary conditions become important.  
 8 The Dominant Periodicities (DP) are marked in an arrow. DPs are a statistically  
 9 significant region of the wavelet spectrum within a band of lower  
 10 frequencies/periodicities. It is emphasized that these higher power regions extend in  
 11 time and are not very local features in the power spectrum.

12  
 13  
 14  
 15  
 16  
 17  
 18



1 **Figure 2** Same as Figure 1 but for the sun-spot number time series (SILSO, World Data  
 2 Center). Dominant Periodicities (DP) are marked in arrows.

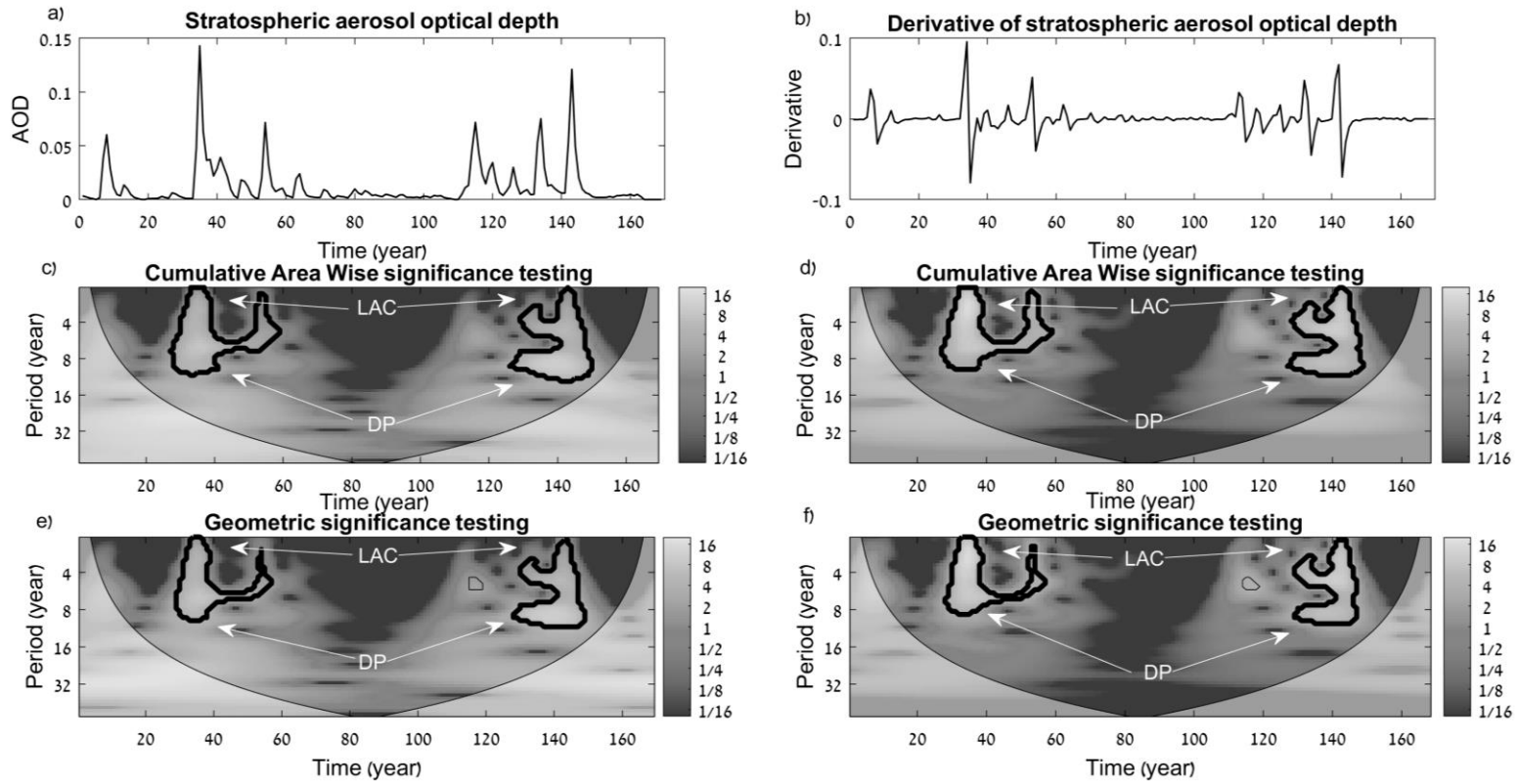
- 3
- 4
- 5
- 6
- 7
- 8
- 9
- 10
- 11
- 12
- 13
- 14
- 15
- 16
- 17
- 18



1 **Figure 3** Same as Figure 1 but for a Local Abrupt Change time series. Local Abrupt  
 2 Changes (LAC) and Dominant Periodicities (DP) are marked in arrows.

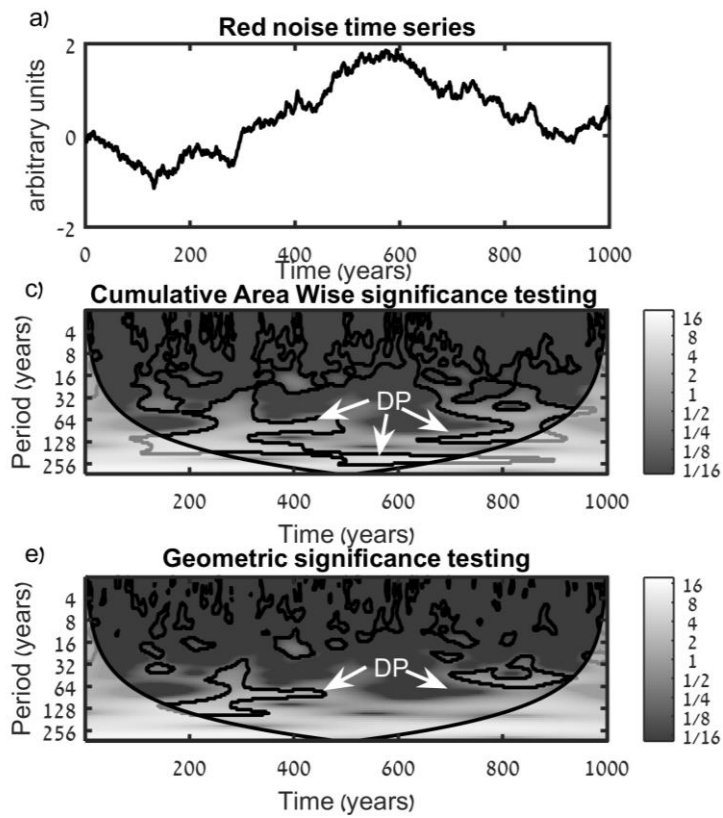
- 3
- 4
- 5
- 6
- 7
- 8
- 9
- 10
- 11
- 12
- 13
- 14
- 15
- 16
- 17





1 **Figure 4** Same as Figure 1 but for the stratospheric aerosol optical depth time series  
 2 (Bourassa *et al.*, 2012). Local Abrupt Changes (LAC) and Dominant Periodicities (DP)  
 3 are marked in arrows.

- 4
- 5
- 6
- 7
- 8
- 9
- 10
- 11
- 12
- 13
- 14
- 15
- 16
- 17
- 18



1 **Figure 5** Same as Figure 1 but for a red noise time series.

2

3

4

5

6

7

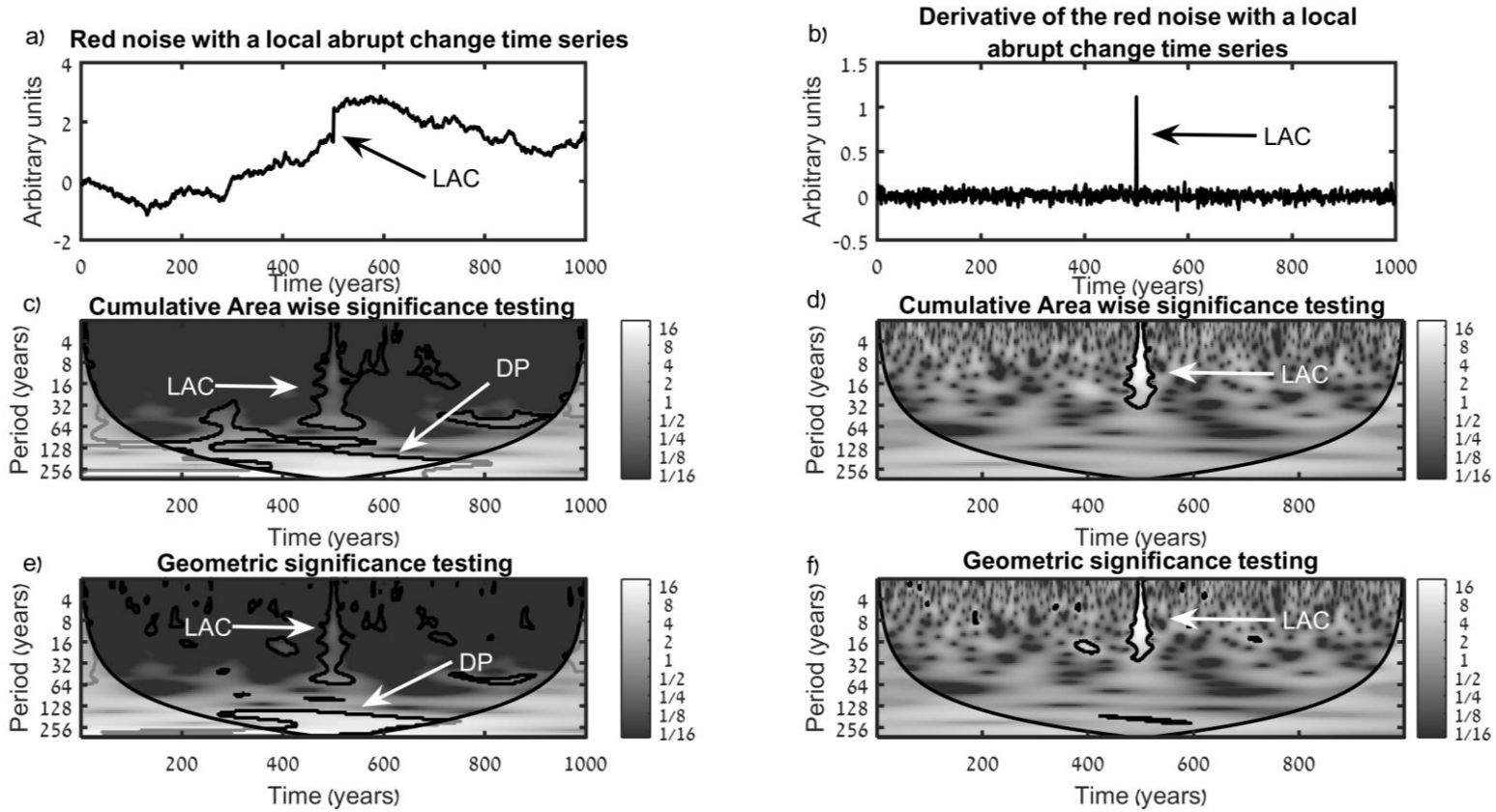
8

9

10

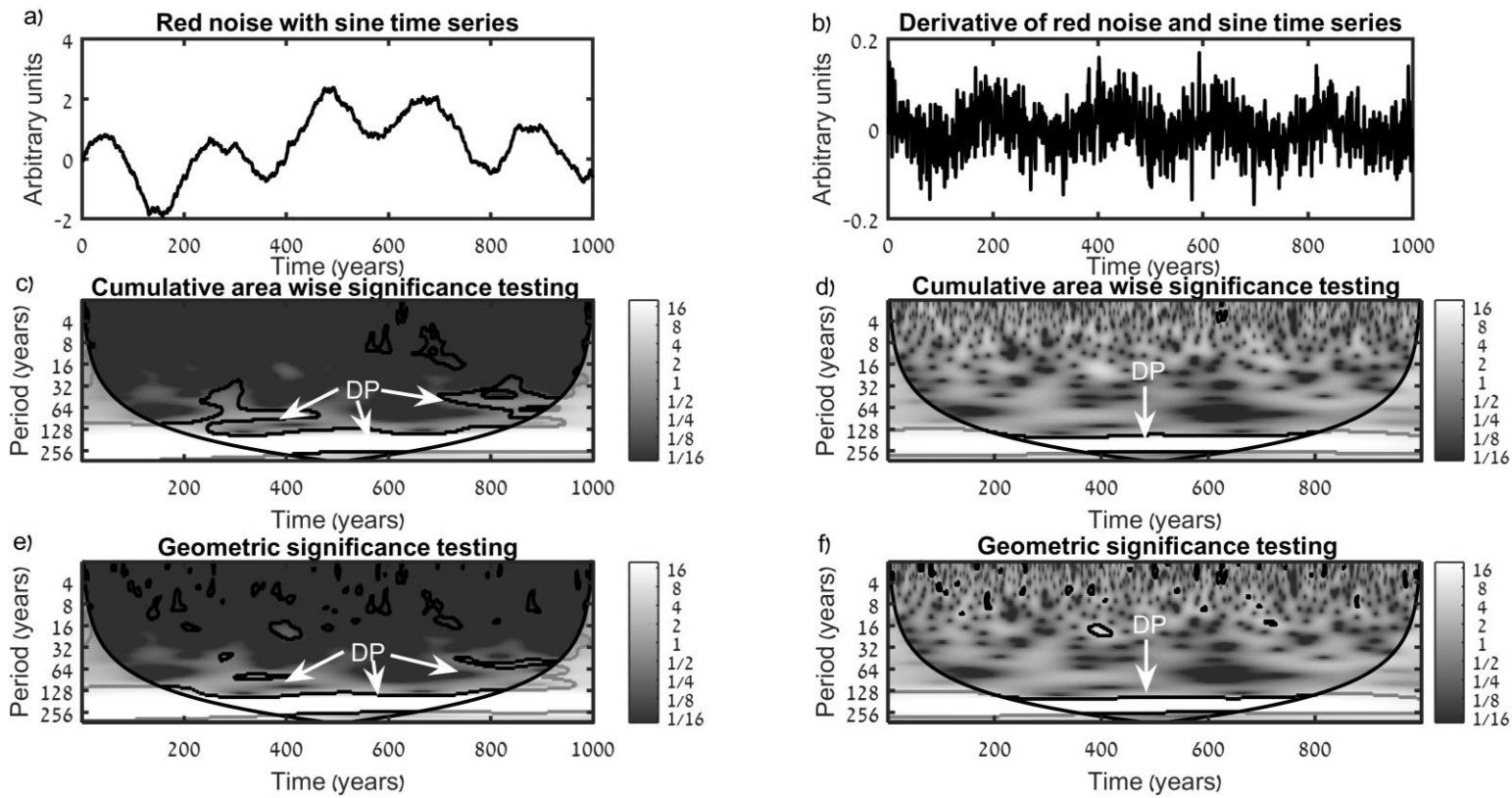
11

12



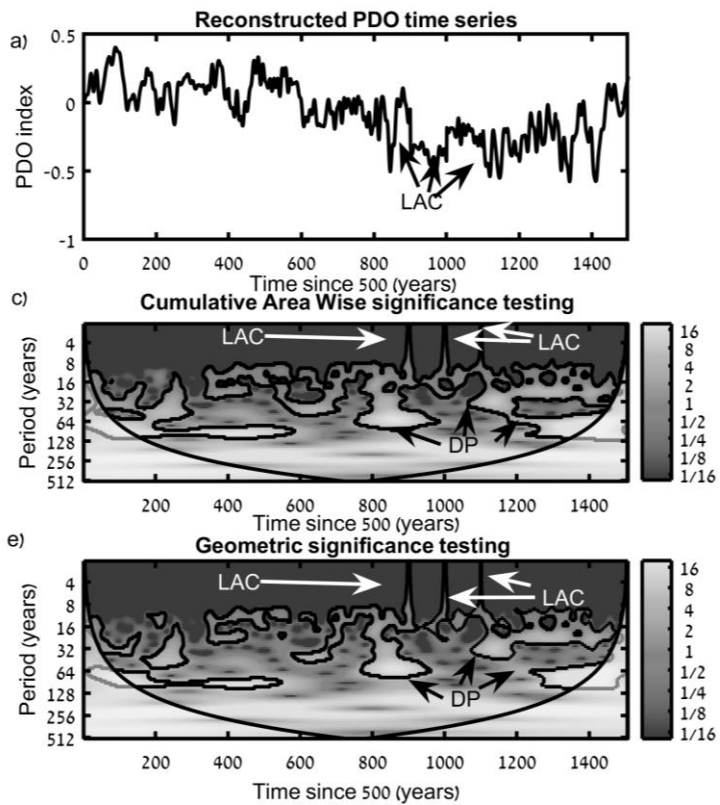
1 **Figure 6** Same as Figure 1 but for the red noise time series added to the Local Abrupt  
 2 Change (LAC) time series. LAC and Dominant Periodicities (DP) are marked in arrows.

- 3
- 4
- 5
- 6
- 7
- 8
- 9
- 10
- 11



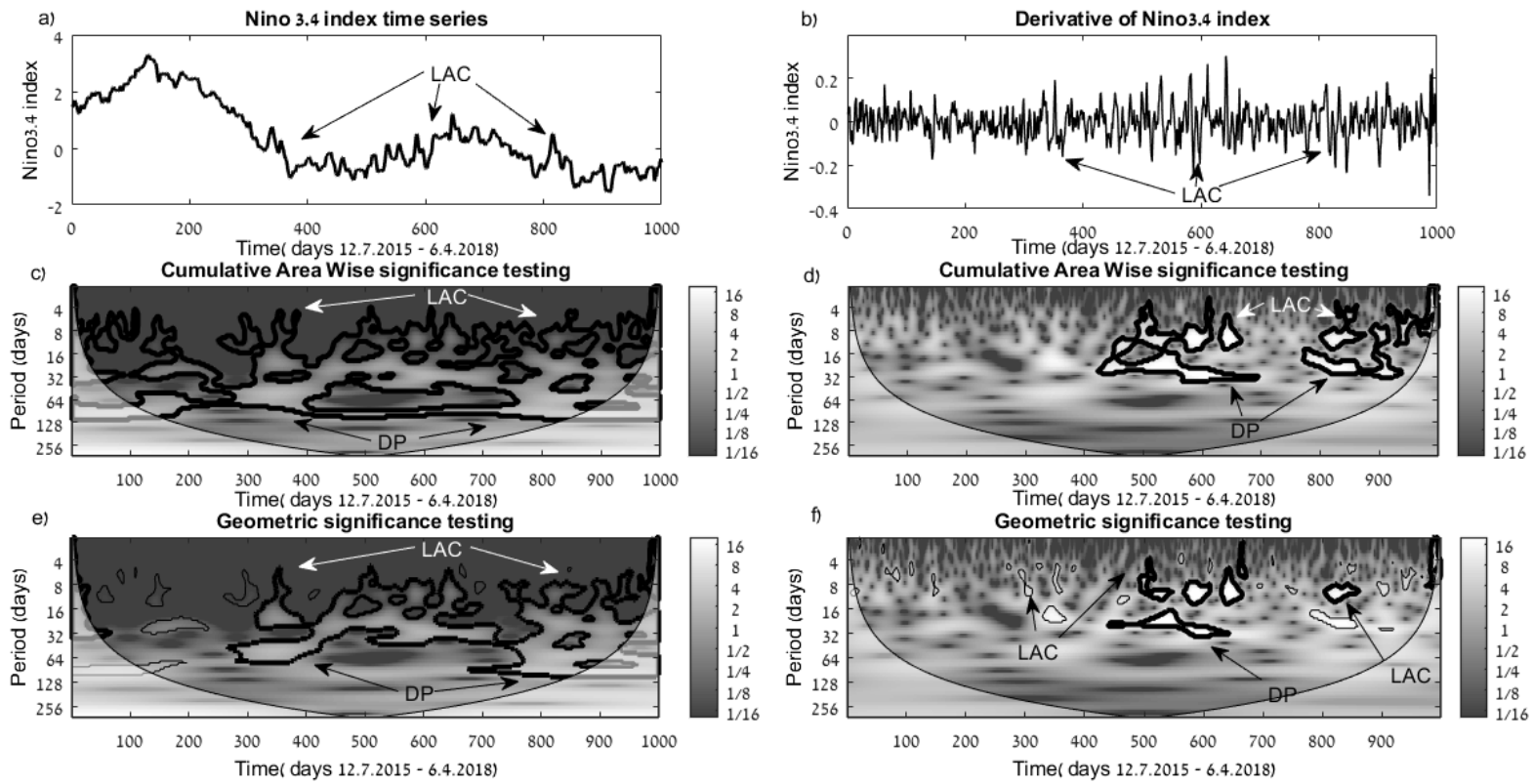
1 **Figure 7** Same as Figure 1 but for the sine time series added to the red noise time series.  
 2 Dominant Periodicities (DP) are marked in arrows.

- 3
- 4
- 5
- 6
- 7
- 8
- 9
- 10
- 11
- 12
- 13
- 14
- 15
- 16
- 17



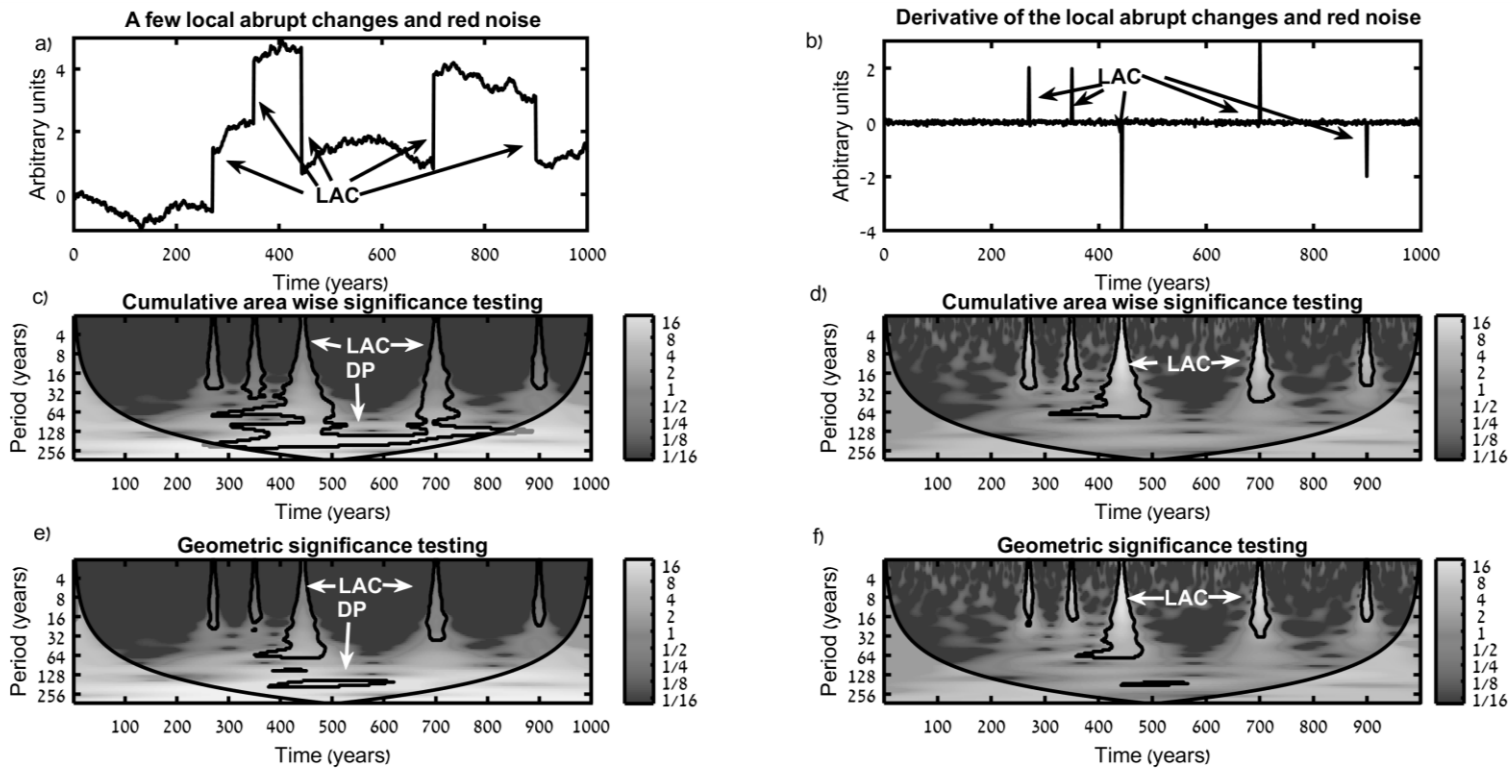
1 **Figure 8** Same as Figure 1 but for the reconstructed PDO (Mann *et al.*, 2009). Local  
 2 Abrupt Changes (LAC) and Dominant Periodicities (DP) are marked in arrows.

- 3
- 4
- 5
- 6
- 7
- 8
- 9
- 10
- 11
- 12
- 13
- 14
- 15



1 **Figure 9** Same as Figure 1 but for the Nino3.4 index 12.7.2015 – 6.4.2018. Local  
 2 Abrupt Changes (LAC) and Dominant Periodicities (DP) are marked in arrows.

- 3
- 4
- 5
- 6
- 7
- 8
- 9
- 10
- 11
- 12
- 13
- 14
- 15
- 16
- 17
- 18



- 1 **Figure 10** Same as Figure 1 but for a time series with a few Local Abrupt Changes
- 2 (LAC) added to red noise.
- 3